INL/CON-11-21793
PREPRINT

Microstructure, Processing, Performance Relationships for High Temperature Coatings

25th Annual Conference on Fossil Energy Materials

Thomas M. Lillo

April 2011

The INL is a
U.S. Department of Energy
National Laboratory
operated by
Battelle Energy Alliance

Microstructure, Processing, Performance Relationships for High Temperature Coatings

Thomas M. Lillo
Idaho National Laboratory, P.O. Box 1625, MS 2218, Idaho Falls, ID 83415-2218

Abstract

This work evaluates the suitability of iron aluminide coatings for use in high temperature fossil fuel combustion environments, such as boiler applications. The coatings are applied using High Velocity Oxy-Fuel (HVOF) thermal spray techniques. Iron aluminide coatings, with the nominal composition of Fe_3Al, were applied to various high temperature structural materials (316 Stainless Steel, 9Cr-1Mo steel and Inconel 600) that typically lack inherent resistance to environmental degradation found in fossil fuel combustion atmospheres. Coating/substrate combinations were subjected to thermal cycling to evaluate the effect of HVOF parameters, coating thickness, substrate material and substrate surface roughness on the resistance to coating delamination and cracking. It was found that substrate surface roughness had a profound influence on the performance of a given substrate/coating system and that surface preparation techniques will need to be tailored to the specific substrate material. Also, higher particle velocity during HVOF thermal spray deposition of the iron aluminide coatings tended to result in better-performing coating/substrate systems with less delamination at the coating/substrate interface. Some combinations of HVOF parameters, coating thickness and substrate materials were found to perform extremely well even at temperatures up to 900°C. However, in some cases, substantial reactions at the interface were observed.

Introduction

The key to increasing the efficiency and reducing emissions, of fossil power plant is to increase the operating temperature. There has been a steady increase in fossil fuel fired power plant operating temperatures – 530-560°C for many current fossil fuel power plants [1], as high as 600°C for some current advanced plants [2] and up to 760°C for the proposed advanced, ultra-supercritical power plant [3, 4]. These systems are limited by the high temperature mechanical properties and corrosion resistance of the materials in combustion environments. The high operating pressure (>13 MPa) inside super-critical and ultra-supercritical systems necessarily require creep resistance of the structural materials. Often times, materials that satisfy the high temperature, structural requirements do not possess the required corrosion resistance. However, application of corrosion resistant coatings onto these high temperature structural alloys offers a means of satisfying both the structural and environmental requirements in high temperature fossil energy applications.

This work seeks to develop iron aluminide coatings, specifically, Fe_3Al coatings, for use in fossil fuel combustion atmospheres. While Fe_3Al has been shown to be highly corrosion resistant in simulated fossil fuel combustion atmospheres [5,6], its bulk mechanical properties make is unsuitable in high temperature structural applications [7]. Iron aluminide powder is readily available and the High Velocity Oxy-Fuel (HVOF) thermal spray coating technique is capable of controlling the residual stress in the coating, through manipulation of the quenching stress, coating/substrate CTE mismatch and the "peening" stress, to generate coatings with a high durability. The powder particles during HVOF coating application are typically semi-solid and moving at many hundreds of meters/second. These semi-solid particles can cause significant deformation of the substrate surface upon impact, effectively "peening" the surface.

(The peening stress that develops during HVOF is absent or insignificant in the various other types of coating techniques, e.g. plasma spray, twin wire arc spraying, aluminizing, CVD, etc..) The relative contributions of the quenching, peening and CTE mismatch stresses sum to give the residual stress state in the coating that can range from tensile to neutral to compressive [8,9] and is largely controlled by the combustion chamber pressure in the HVOF thermal spray gun. A compressive stress state is most desirable for relatively brittle iron aluminide coatings, since tensile stresses in the coating would tend to promote cracking.

Iron aluminide coatings generally fail by mechanical means – cracking, delamination, spalling – rather than by corrosion mechanisms since Fe_3Al has good corrosion resistance in fossil fuel combustion atmospheres. Therefore, HVOF Fe_3Al coatings have been mainly evaluated through rapid thermal cycling to temperatures relevant to the expected operating temperature. The results of the thermal cycling tests performed on Fe_3Al coatings applied with HVOF thermal spray techniques to 316 SS, 9Cr-1Mo steel and Inconel 600 are reported here to gain an understanding of the influence of various parameters on the resulting durability of the coating/substrate system. The thermal spray combustion chamber pressure, the coating thickness, the substrate temperature rise during deposition and the thermal cycling temperature were the main parameters of interest in this study.

Experimental Methods

Thermal cycling experiments were performed on coated substrates in which the thermal spray combustion chamber pressure was held constant - coating thickness and substrate thickness were varied – or the coating thickness was held constant - the thermal spray combustion chamber pressure was varied. For the former condition, Fe_3Al coatings of various thicknesses were applied to thick plates (12.7 mm or 19.1 mm thick, carbon steel or 9Cr-1Mo steel plates) at constant thermal spray combustion chamber pressure (P_C= 0.6 MPa). In the latter condition, rods, 12.7 mm in diameter, were coated at two different chamber pressures (0.6 MPa and 0.3 MPa) to a nominal coating thickness of 250 microns. Three different rod materials were used as substrates – 316SS, 9Cr-1Mo steel and Inconel 600. The first two are iron-based while the last one is a high temperature nickel-based alloy.

Surface Preparation of the Substrates – Preparation of the substrate surface for subsequent coating deposition consisted of degreasing with alcohol followed by automated grit blasting for both plate- and rod-type substrates. The abrasive media was 24-grit (700 micron) Alundum (Norton St. Gobain) and the grit blasting parameters were: 480 kPa air pressure, 6.4 mm diameter nozzle and a 25 mm standoff distance. The nozzle was rastered across the surface of the plates with a traverse speed of 10 mm/second and the pitch was 7 mm. The rod-type substrates were rotated with a surface velocity of 10 mm/second and traverse speed of 4 mm/second. After grit blasting the surfaces were blown off with compressed air to remove debris. The resulting surface roughness of each substrate material was measured with a Wyko NT1100 Optical Profiling System.

HVOF Fe_3Al Coating Deposition – The composition of the powder used for HVOF coating deposition is shown in Table 1 and corresponds to Fe_3Al with minor additions of chromium and zirconium for enhanced mechanical properties. The particle size of the powder was -270 US Standard Mesh Size with the majority of the powder (>80%) being -400 US Standard Mesh Size. The HVOF torch parameters are shown in Table 2. The surface of the plate substrate was rastered in front of the HVOF torch at a rate of 100

Table 1 Composition of the Iron Aluminide Powder

Supplier: AMETEK Product: FAS-C (-270) Lot #: 037601					
Element	Fe	Al	Cr	Zr	C
Wt. %	Bal.	15.7	2.4	0.2	0.02

mm/sec with 5 mm pitch. Rods were traversed in front of the torch at a rate of 10 mm/second while being rotated at 10 revolutions per second. The temperature of plate-type substrates was monitored during coating deposition with a thermocouple inserted into a blind hole in the back of the substrate. The junction was located within approximately 3 millimeters of the surface being coated. The temperature of the rod substrates during deposition was not measured due to the rotation of the rod. Compressed air was applied to the front of all substrates to moderate substrate heating during thermal spray deposition, unless otherwise noted.

Table 2 HVOF Thermal Spray Parameters

HVOF Thermal Spray Torch	JP 5000, 10.2 cm barrel	
Standoff distance	35.6 cm	
Chamber pressure	0.6 MPa	0.3 MPa
Kerosene flow rate	26.5 l/h	16.7 l/h
Oxygen flow rate	820 slm	520 slm
Equivalence Ratio	1	1
Powder	Fe_3Al, Lot #0376601	
Carrier gas flow rate	5 slm	
Rotation	5 rpm	

Thermal Cycling - Samples, 12.7 mm in diameter were EDM-machined from relatively thick plates (12.7 and 19.1 mm thick) coated at constant chamber pressure (P_c= 0.6 MPa). The samples were then placed in quartz tubes, evacuated, backfilled with a ¼ atmosphere of UHP argon and sealed. A CM Sealed Box Furnace, Model 1720 SM(C)) and a vertical tube furnace (Thermolyne Tube Furnace, Model F79300) were used to thermally cycle sets of samples at different temperatures up to 700°C. The temperature schedule consisted of heating to the maximum cycle temperature in one hour, a one hour hold at this temperature and furnace cooled to less than 90°C (approximately 1 hour). The samples were cycled 100 times and then removed from the furnace. The coatings were examined through the quartz tube for evidence of coating delamination. (Delamination of the coating was considered to be coating failure.) The ampoules were returned to the furnace cycled an additional 100 cycles and reexamined. The process was repeated until 500 cycles had been attained. The ampoules were then broke open and the coatings examined for delamination and cracking using dye penetrant techniques.

Various thermal spray combustion chamber pressures were used to apply coatings to 12.7 mm diameter rods of the substrate materials. These coated rod specimens were subjected to rapid thermal cycling using the electrical resistance heating capability of the Gleeble 1500. The uncoated ends of the rods were secured in the water-cooled grips of the Gleeble and a control thermocouple was spot welded to the coating in the center of the sample. High current, electrical resistance heating, in combination with the water cooled grips, allowed very rapid heating and cooling - typically, 1.5 minutes to the cycle temperature, a 2 minute hold time and then cooling for 4 minutes before the next cycle was started. In general, heating rates ranged from 367°C/ minute to 600°C/minute - much greater than those in the tests (~10°C/minute) on the plate material described above. After 250 cycles, each sample was scanned for through thickness cracking using eddy current methods. The sample was then cycled an additional 250 cycles and re-scanned for through-thickness cracking.

Microstructural Examinations – After testing, all samples that did not show obvious signs of coating failure were sectioned and the coating/substrate interface examined in detail for signs of delamination and through thickness cracking. Optical metallography was used to evaluate the coating thickness and microstructure. Image analysis was used to assess the fractional amount of coating porosity.

Experimental Results

Substrate Surface Roughness – Although the surface of all the substrate materials were prepared using the same grit blasting parameters, a potential existed for significantly different surface roughness to develop

on the various substrate materials due to differences in material hardness and other material-specific mechanical properties. Therefore, the surface roughness of each of the substrate materials was measured after grit blasting. Table 3 shows significant differences exist in the surface roughness produced by grit blasting the four different materials. The 9Cr-1Mo steel and carbon steel exhibit the lowest surface roughness after grit blasting while Ni-based Inconel 600 and 316 SS exhibit significantly greater surface roughness.

Table 3 Substrate Roughness

Grit Blasted Substrate	R_{RMS}, microns	R_t, microns
9Cr-1Mo steel	7.24	59.24
Carbon steel (1018)	7.65	58.75
316 Stainless Steel	7.73	81.62
Inconel 600	8.23	81.91

Substrate Temperature During HVOF Coating and Resulting Coating Thickness – The substrate temperature as a function of successive coating layers for carbon steel and 9Cr-1Mo steel plate-type substrates during HVOF coating deposition is shown in Fig. 1a & 1b, respectively. The temperature increases with each additional layer applied during HVOF deposition and appears to approach an equilibrium value when more than 3 layers were applied.

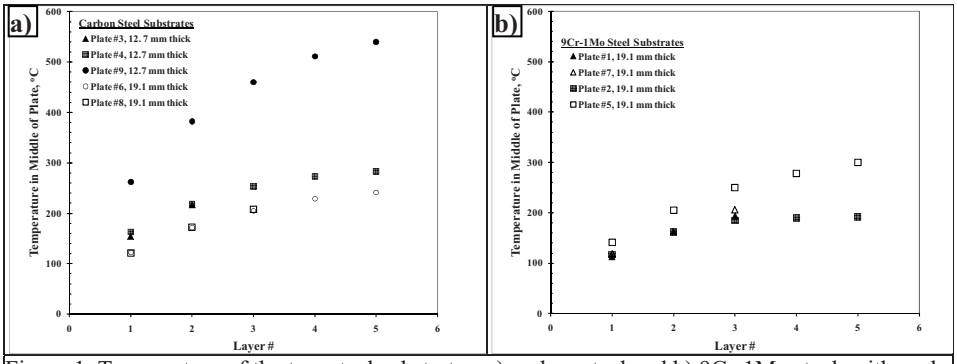

Figure 1. Temperature of the two steel substrates, a) carbon steel and b) 9Cr-1Mo steel, with each successive layer of Fe_3Al applied by HVOF.

This equilibrium deposition temperature appears to be a function of substrate thickness, substrate material and whether cooling air was applied to the plate during deposition. The maximum temperature attained in the substrate during HVOF coating deposition generally ranged from 200-300°C, although it was drastically higher (~540°C) when cooling air was not applied to the front face of the substrate, Plate #9 in Fig. 1a. The maximum temperature attained by the substrate increases as the number of coating layers applied increases. The thickness of the substrate, either 12.7 mm or 19.1 mm thick, had a much smaller, though noticeable, effect on the carbon steel substrate temperature, Fig. 1a. The difference in maximum temperature between substrates 12.7 mm thick and 19.1 mm thick was less than 50°C with thicker substrates experiencing a smaller temperature rise.

The final coating thickness is directly related to the number of layers applied, Fig. 2. There is only a small difference in final coating thickness between the carbon steel and the 9Cr-1Mo steel specimens. However, the maximum substrate temperature attained during deposition appears to have a small influence on the final coating thickness. For a 12.7 mm thick carbon steel substrate, 5 layers produce a final coating thickness of around 400 microns when cooling air is applied (T_{Max}= 280°C) versus ~360 microns in the absence of cooling air (T_{Max}= 540°C).

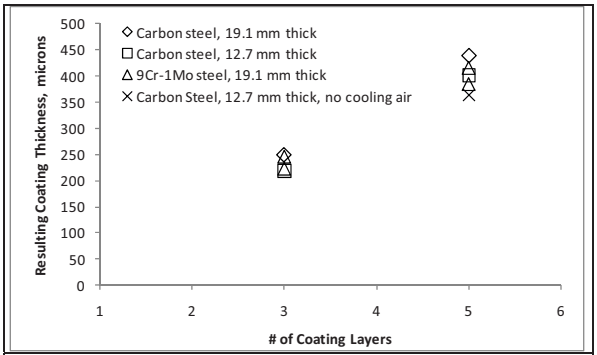

Figure 2. Coating thickness increases with increasing number of layers applied.

Coating Microstructure -The microstructure of the coatings that develops using thermal spray combustion chamber pressures, P_c, of 0.3 MPa and 0.6 MPa are shown in Fig. 3 for the 9Cr-1Mo steel

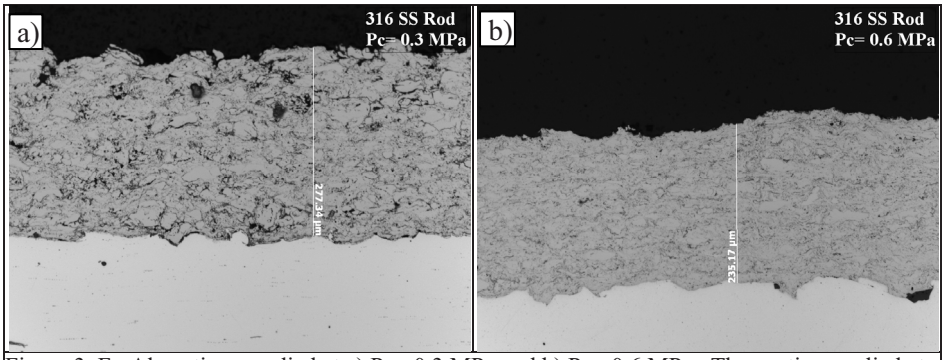

Figure 3. Fe_3Al coatings applied at a) P_C= 0.3 MPa and b) P_C= 0.6 MPa. The coating applied at P_C= 0.3 MPa exhibits more porosity – 2% vs. 0.4% for P_C= 0.6 MPa.

rod-type substrate materials. In general, the coatings conform very well to the grit blasted substrate surface, Fig. 3. A greater level of porosity was observed when the coatings were applied at the lower chamber pressure, P_C= 0.3 MPa, on the order of 2% versus ~0.4% when applied at P_C= 0.6 MPa. However, the density of voids at the interface in all samples was low, indicating the particle velocity and temperature associated with both chamber pressures appeared to be sufficient to efficiently extrude the particles into the rough substrate surface and provide good mechanical bonding. Also, the substrate material, substrate temperature and coating thickness had a negligible effect on the resulting microstructures which were all similar to those in Fig. 3.

Thermal Cycling Behavior – Combustion Chamber Constant, P_C= 0.6 MPa – Fe_3Al coatings, ranging from 200 to 400 microns thick, on carbon steel and 9Cr-1Mo steel plate substrates were thermally cycled at temperatures up to 700°C for a total of 500 cycles. The substrate temperature during HVOF coating deposition in this sample set ranged from about 190 to about 300°C, while the one carbon steel substrate without air cooling experienced temperatures as high as 540°C. The results of thermal cycling are shown in Fig. 4. The coatings were checked for delamination every 100 thermal cycles and, to be conservative, the minimum number of cycles completed without failure was reported here (i.e., if the coating was not delaminated after 300 cycles but was after 400 cycles the minimum number of cycles to failure was reported as 300 cycles). The minimum number of cycles completed without failure has been plotted as a function of both final coating thickness and the temperature measured in the substrate during deposition. In the case of Fe_3Al on carbon steel, increasing coating thickness does not necessarily result in poorer performance, at least not at the lowest thermal cycling temperature of 620°C. Although, at a thermal cycling temperature of

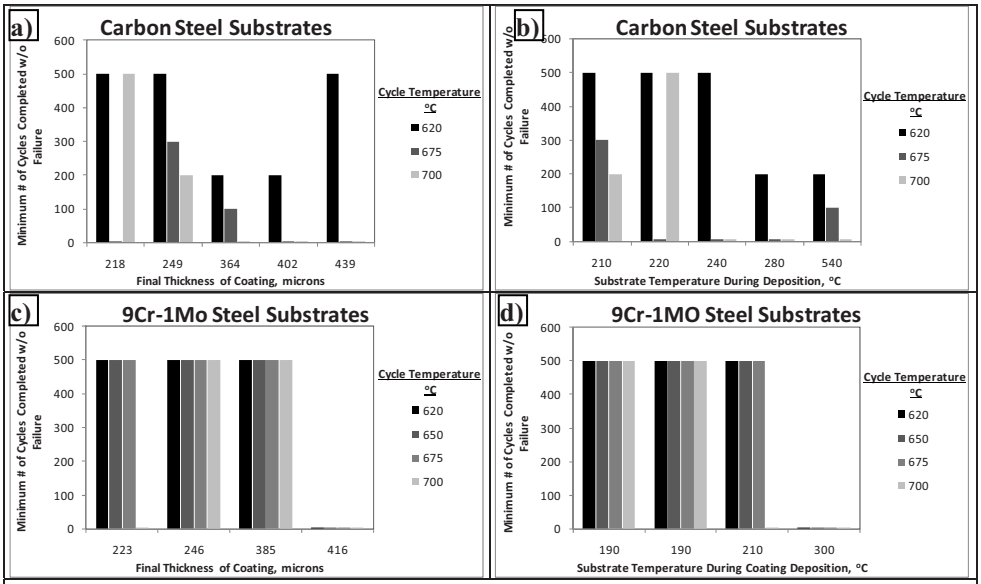

Figure 4. Summary of the thermal cycling results for coatings applied at constant combustion chamber pressure (P_C= 0.6 MPa). Lower thermal cycling temperatures, thinner coatings and lower substrate temperatures during deposition resulted in better performance.

700°C it does appear that poorer performance is associated with thicker coatings. Alternatively, when plotting the cycling behavior as a function of substrate temperatures during deposition, reduced performance at all thermal cycling temperatures appears to be associated with higher substrate deposition temperatures. Conversely, Fe_3Al coatings on 9Cr-1Mo steel showed good performance at all except the thickest coatings and the highest substrate temperatures attained during deposition.

Thermal Cycling Behavior – Coating Thickness Constant, t= 260 microns – Fe_3Al coatings, applied at a combustion chamber pressure of either 0.3 MPa or 0.6 MPa, were sprayed on to 9Cr-1Mo steel, Inconel 600 and 316 Stainless Steel rod-type substrates to a thickness of approximately 260 microns. Thermal cycling was carried out in the Gleeble and was very rapid to reduce testing time while still being able to resolve differences in coating behavior. In this set of experiments, the samples were examined for failure every 250 thermal cycles. The results were report simply as pass/fail – coatings that did not crack or delaminate during 500 thermal cycles were considered to have "passed". The results are summarized in Fig. 5. Coatings applied to 9Cr-1Mo rod substrates performed poorly and only the sample cycled at

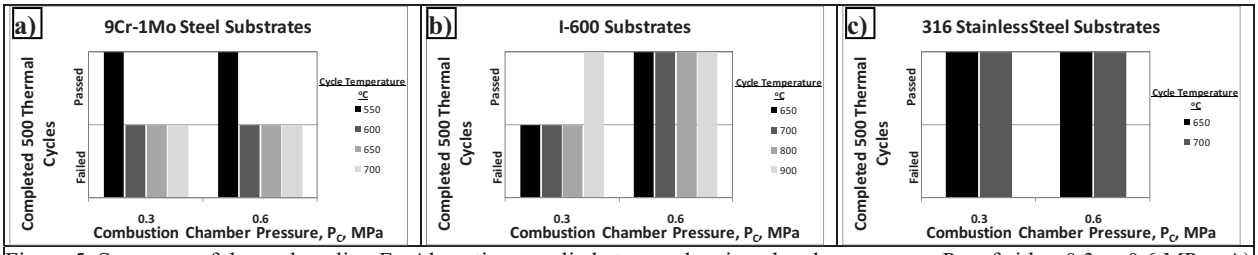

Figure 5. Summary of thermal cycling Fe_3Al coatings applied at a combustion chamber pressure, P_C, of either 0.3 or 0.6 MPa. A) Coatings on 9Cr-1Mo steel substrates performed poorly while coatings on b) Inconel 600 performed well only when P_C = 0.6 MPa. C) Coating performance on 316 Stainless Steel was insensitive to P_C. The failure criterion was 500 thermal cycles without delamination or through-thickness cracking.

the lowest temperature (550°C) survived 500 thermal cycles – all others failed regardless of what combustion chamber pressure was used to apply the coating. However, the coatings applied to Inconel 600 did show an effect of combustion chamber pressure. All these samples coated at the higher combustion chamber pressure survived 500 cycles while coatings applied at the lower chamber pressure failed, except the sample cycled at the highest cycling temperature of 900°C. Coatings of Fe_3Al applied to 316 SS performed very well and no effect of combustion chamber pressure on performance was observed.

Microstructural Observations After Thermal Cycling – After thermal cycling various samples were sectioned and prepared for optical metallography. In general, the microstructure of the coating was unchanged after exposure to the thermal cycling temperatures, Fig. 6. Coating

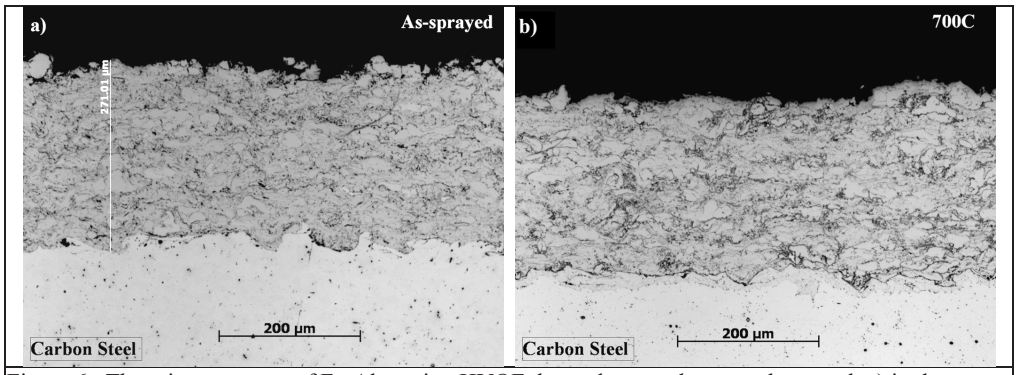

Figure 6. The microstructure of Fe_3Al coating HVOF thermal sprayed onto carbon steel, a) in the as-sprayed condition and b) after 500 thermal cycles to 700°C. No significant changes to the microstructure are observed due to high temperature cycling.

failure mainly occurred by delamination, although two instances of through thickness cracking were observed in coatings applied at P_C= 0.3 MPa (no through-thickness cracking was observed in coatings applied with P_C= 0.6 MPa – only coating delamination), Fig. 7. And finally, significant interfacial reactions were observed only in a two samples cycled to the highest temperatures, 900°C. The reaction in the carbon steel appeared to be mainly precipitation along grain boundaries near the surface while the reaction in the Inconel 600 was much more extensive with inter-diffusion through the coating on the order of 20 microns. The penetration rates are estimated to be on the order of 10-20 nm/hour in the carbon steel at 700°C and 1.2 microns/hour for the Inconel 600 at 900°C.

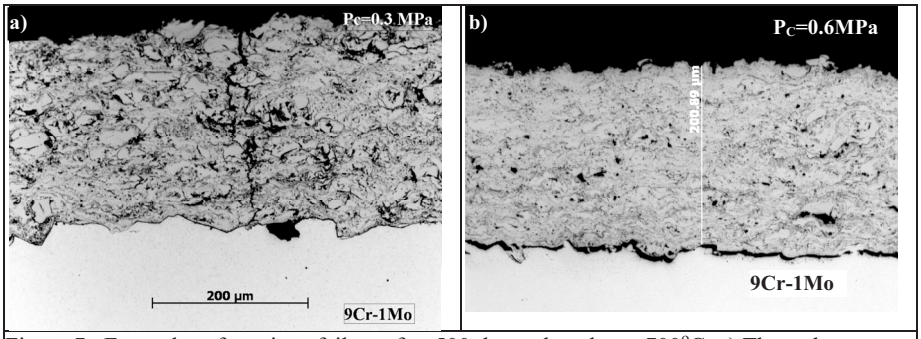

Figure 7. Examples of coatings failure after 500 thermal cycles at 700°C: a) Through thickness cracking in the Fe_3Al coating applied at P_C=0.3 MPa and b) Delamination of Fe_3Al coating from the underlying 9Cr-1Mo substrate, P_C= 0.6 MPa.

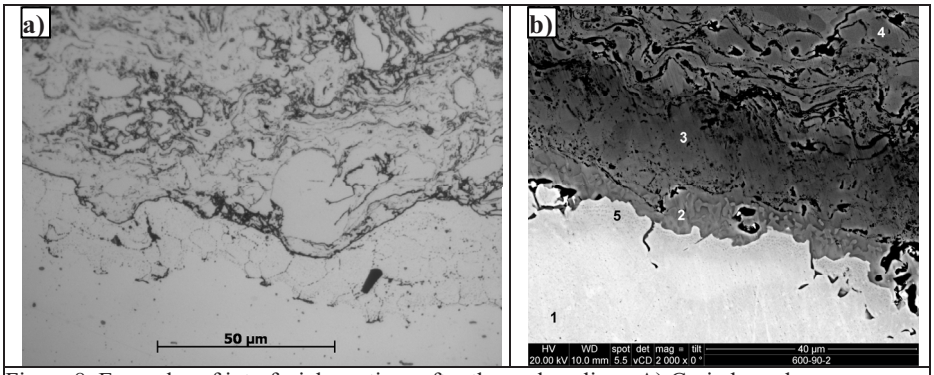

Figure 8. Examples of interfacial reactions after thermal cycling. A) Grain boundary precipitation in the carbon steel substrate, 500 thermal cycles @ 700°C and b) diffusion of nickel from the Inconel 600 substrate into the coating after 500 thermal cycles at 900°C.

Discussion

In general, bonding of thermal spray coatings to the substrate is largely mechanical with little atomic or chemical bonding at the interface. Ultimately, stresses at the interface cause the coating to fail by either delaminate or spallation. Residual stresses in the coating arise during deposition and can be used to offset thermal stresses that arise at the test temperature due CTE mismatch between the coating and the substrate. As mentioned the residual stress in the coating is a combination of the quenching stress due to the solidification of molten material during deposition, the peening stress due to deformation caused by high velocity impacts of the solid fraction during deposition and the CTE mismatch between the coating and substrate, the magnitude of which is determined by the substrate temperature during deposition. The sample sets and HVOF thermal spray parameters were chosen to explore the effect of these parameters on coating durability.

Table 4 Coefficients of Thermal Expansion

Material	Coefficient of Thermal Expansion, ppm/°C
Carbon Steel (1018)	14
316 Stainless Steel	18
9Cr-1Mo (Grade 91)	13
Inconel 600	15
Fe_3Al - wrought	20.5
Fe_3Al - Coating, P_c=0.3 MPa	13
Fe_3Al - Coating, P_c=0.6 MPa	12

Substrate Temperature During Deposition – Substrate temperature during deposition contributes to the residual stress through CTE mismatch between the coating and substrate. Stresses arise when the coating/substrate system is cooled after deposition or when it is raised above the deposition temperature to the test temperature. Table 4 shows

the CTE for the various materials in this work. The Fe_3Al coatings, whether applied with P_C- 0.3 or 0.6 MPa, exhibit quite low CTEs compared to wrought Fe_3Al due to the inclusion of oxides in the coating [10]. In general, all the substrates have CTEs that exceed that of the coating. Therefore, the CTE mismatch adds a compressive component to the coating upon cooling after deposition. However, raising the coating/substrate system above the deposition substrate temperature will result in a tensile component due to the CTE mismatch. Systems that attained the highest substrate temperatures during deposition should experience the smallest tensile component due to CTE mismatch and, therefore, should be less likely to fail by delamination or spalling. However, this trend does not appear to be followed in the plot of Fig. 4b for carbon steel substrates which shows that coatings tend to fail with *increasing* substrate deposition temperature. It has been shown previously that the residual stress in the coating is independent of coating thickness [8] and, therefore, the influence of coating thickness on durability is expected to be negligible and no clear trends are observed in Fig. 4a.

The 9Cr-1Mo steel substrate is not expected to exhibit a durability strongly influenced by the deposition temperature or the thermal cycling temperature. The CTE mismatch of Fe_3Al on 9Cr-1Mo steel is virtually zero and not significant thermal stress due to CTE mismatch should develop. This would appear to be demonstrated in Fig. 4d. However, the coating deposited at the highest temperature on to 9Cr-1Mo steel still preferentially fails compared to coatings applied at lower temperatures, Fig. 4d.

CTE of the Substrate Materials – As mentioned, the CTEs of all the substrates meet or exceed the CTE of the Fe_3Al coatings. As the thermal cycling temperature is increased the stress within the coatings should be become increasingly tensile and facilitate crack initiation and propagation. Thus one would expect the substrate/coating systems with the highest CTE mismatch to be more likely to fail than substrate/coating system with lower values CTE mismatch, especially as the thermal cycling temperature increases. Thus, one would expect the coating on 316 SS to exhibit the lowest durability since it exhibits the highest CTE mismatch of all the substrate/coating systems. However, the results in Fig. 5 tend to indicate that durability *increases* with increasing CTE mismatch. It appears that factors other than CTE mismatch are playing a critical role in the observed durability of the coating on the different substrates.

Thermal Spray Combustion Chamber Pressure, P_C, - The combustion chamber pressure, P_C, directly affects the velocity of the particles during thermal spray deposition. Previous work with this HVOF thermal spray equipment [10] has shown that combustion chamber pressures of 0.3 and 0.6 MPa result in an average particle velocity of 570 and 630 m/sec, respectively. A direct effect of the increased particle velocity is the lower measured porosity at the higher value of P_C, 0.4% vs. 2% at P_C=0.3 MPa. Faster moving particles are better able to deform and fill void space.

Increasing the combustion chamber pressure also has been shown to dramatically increase the residual stress in the coating due to the increased peening action of the particles at the higher velocity [10]. This peening stress is compressive and resists crack initiation. Therefore it is expected that coatings applied at the higher values of P_C generally tend to exhibit better durability which appears to the case for Fe_3Al applied to Inconel 600, Fig. 5b. However, coatings applied to 9Cr-1Mo steel performed poorly regardless of the value of P_C. Conversely, the coatings on 316 SS perform very well, again, regardless of the value of P_C. The initial surface roughness may be the root cause of the difference in behavior since the 9Cr-1 Mo steel exhibited the lowest surface roughness while the 316 SS and the Inconel 600 surfaces were considerably rougher. It is also possible that the peening action may affect the surface roughness – effectively reducing the roughness – or that the different substrates "peen" differently (e.g. the 9Cr-1Mo steel rod has a significantly higher yield stress than that of either Inconel 600 or 316SS) and give rise to

different residual stress states and the different observed durability. From this work the influence of combustion chamber pressure on durability is not entirely clear.

Surface Roughness – One particularly important parameter is the surface roughness of the substrate. Since the particles are at least partially molten during HVOF thermal spray deposition they tend to conform well to the surface onto which they are sprayed. Therefore, coating bond strength is greatly influenced by interfacial area. Rougher surfaces have greater interfacial area and typically exhibit greater coating bond strength. In this work, all the substrates were prepared by automated grit blasting and, therefore, all substrate surfaces experienced equivalent surface preparation. However, Table 3 shows that the resulting substrate roughness is a sensitive function of the substrate material and is undoubtedly due to the inherent mechanical properties of the substrate material (e.g. yield strength, strain rate hardening, ductility, etc.). The 9Cr-1Mo steel substrate is tempered martensite, exhibiting a relatively high yield strength and limited ductility at room temperature while the other substrates typically exhibit lower yield strength and greater ductility. Therefore, it is not surprising that the 9Cr-1Mo steel substrate exhibits the lowest value of surface roughness after grit blasting. Based solely on substrate roughness, one would expect the bond strength to be greatest for the 316 Stainless Steel and the Inconel 600 substrates and significantly reduced in the 9Cr-1 Mo substrates. Figure 5 seems to confirm this assumption with coatings on 316 SS and Inconel 600 exhibiting better durability than the coatings on the 9Cr-1Mo steel substrate. However, it is somewhat puzzling that Fe_3Al coatings on plates of 9Cr-1Mo steel performed very well, Fig. 4c and 4d, and yet performed quite poorly when the substrate was in rod form, Fig. 5a. However, the plate-type substrates came from hot rolled plate while the rod material was cold drawn and the two materials exhibit a significant difference in the yield strength and hardness. It is possible that differences in either surface roughness or substrate temperature (due to the round geometry and relatively small cross section) or both existed between the two types of substrates. Additional work is being done to determine the substrate type dependence for this material.

Interfacial reactions – Interfacial reactions appear to become a concern at operating temperature over about 700^{o}C. Precipitation at the grain boundaries of carbon steel was observed after 500 cycles at 700^{o}C while significant inter-diffusion of nickel into the Fe_3Al coating was observed on Inconel 600 substrates at a thermal cycling temperature of 900^{o}C. In this work, the reactions did not seem to affect the durability of the coating/substrate systems. However, the exposure time to the elevated temperatures was relatively short (<500 hrs) and brittle phases may form at more extended periods of exposure that could be detrimental to coating adhesion. Furthermore, in the case of the Inconel 600 substrate cycled at 900^{o}C, the reaction may be sufficient to fully consume the coating which may compromise the corrosion resistance of the coating. Longer term exposure experiments will be needed to assess the kinetics of inter-diffusion at temperatures relevant to the intended application(s).

Conclusions

The work over the past year has begun to reveal that various material and HVOF parameters influence the durability of Fe_3Al coatings on prospective high temperature structural materials during thermal cycling to anticipated operating temperatures in fossil fuel applications. Specifically,

- Surface preparation by grit blasting results in a material-specific surface roughness. The grit blasting parameters produced a rougher surface on Inconel 600 and 316 SS substrates than on the 9Cr-1Mo steel substrates.

- Substrates that experienced smaller increases in temperature during HVOF coating deposition seemed to exhibit greater durability – contrary to arguments based on CTE mismatch.
- Substrate/coatings systems with greater CTE mismatch appeared to perform better in thermal cycling experiment – again, contrary to arguments based on CTE mismatch. The thermal cycling results were consistent, however, with the initial surface roughness of the substrate.
- Coatings of Fe_3Al on Inconel 600 survived 500 thermal cycles at temperatures up to 900^{o}C.
- Reactions at the coating/substrate interface can be significant at high thermal cycling temperatures.

Acknowledgements

The author would like to acknowledge the efforts of the many individuals involved in this study. Particularly, great appreciation is extended to W.D. Swank and D.C. Haggard for producing the thermal spray coatings; D.C. Kunerth for performing thermal cycling on the Gleeble 1500 and eddy current measurements; T. Lister for making measurements of surface roughness and T.C. Morris for preparation of numerous metallographic samples.

This work was support by the United States Department of Energy, Office of Fossil Energy, under Department of Energy Idaho Operations Office, Contract No. DE-AC07-05ID14517.

References

[1] Reichel, H.-H., "Fireside corrosion in German fossil-fuel fired power plants. Appearance, mechanisms and causes", Werkstoffe und Korrosion, vol. 39, 1988, pp. 54-63.

[2] Jordal, K., Anheden, M., Yan, J., Stromberg, L., "Oxyfuel combustion for coal-fired power generation with CO2 capture-opportunities and challenges". In: Proceedings of the Seventh International Conference on Greenhouse Gas Control Technologies, Vancouver, Canada, September 2004.

[3] Wright I. G., Maziasz P. J., Ellis F. V., Gibbons T. B., Woodford D. A., " Materials Issues For Turbines For Operation In Ultra-Supercritical Steam", Research sponsored by the U. S. Department of Energy, Office of Fossil Energy, Advanced Research Materials Program, under Contract DE-AC05-00OR22725 with UT-Battelle, LLC., 2004

[4] Maziasz, P.J., Wright, I.G., Shingledecker, J.P., Gibbons, T.B. and Romanowsky, R.R., "Defining of the Materials Issues and Research for Ultrasupercritical Steam Turbines." *Proceedings to the Fourth International Conference on Advances in Materials Technology for Fossil Power Plants(Hilton Head, SC, Oct. 25-28, 2004*). ASM-International, Materials Park, OH, 2005.

[5] Tortorelli, P.F. and DeVan, J.H., "Behavior of Iron Aluminides in Oxidizing/Sulfidizing Environments", Mater. Sci. Eng. A, 1992, A153, pp. 573-577.

[6] Tortorelli, P.F. and Natesan, K., "Critical Factors Affecting the High-Temperature Corrosion Performance of Iron Aluminides", Mater. Sci. Eng. A, vol. A258, 1998, pp. 115-25.

[7] Stoloff, N.S., "Iron aluminides: present status and future prospects", Mater. Sci. Eng. A, 1998, vol. A258, pp.1-14.

[8] Totemeier, T.C, Wright, R.N. and Swank, W.D., "Residual Stresses in High-Velocity Oxy-Fuel Metallic Coatings", Met. & Matls. Trans. A, vol. 35A, 2004, pp. 1807-1814.

[9] Pejryd, L. Wigren, J., Greving, D.J., Shadely, J.R. and Rybicki, E.F., "Residual Stresses as a Factor in the Selection of Tungsten Carbide Coatings for a Jet Engine Application", J. Thermal Spray Technol., vol. 4, 1995, pp. 268-274.

[10] Totemeier, T.C, Wright, R.N. and Swank, W.D., "Microstructure and Stresses in HVOF Sprayed Iron Aluminide Coatings", *J. Thermal Spray Tech*., vol. 11, 2002, pp. 400-408.